

2013

## Dark matter and the mystery of orbital velocities

Joshua Plottel

Joseph Harrison

Follow this and additional works at: <https://digitalcommons.library.uab.edu/inquiro>



Part of the [Higher Education Commons](#)

---

### Recommended Citation

Plottel, Joshua and Harrison, Joseph (2013) "Dark matter and the mystery of orbital velocities," *Inquiro, the UAB undergraduate science research journal*: Vol. 2013: No. 7, Article 23.

Available at: <https://digitalcommons.library.uab.edu/inquiro/vol2013/iss7/23>

This content has been accepted for inclusion by an authorized administrator of the UAB Digital Commons, and is provided as a free open access item. All inquiries regarding this item or the UAB Digital Commons should be directed to the [UAB Libraries Office of Scholarly Communication](#).

## Dark matter and the mystery of orbital velocities

Joshua Plottel<sup>1</sup>, Joseph Harrison<sup>2</sup>

<sup>1</sup>Department of Physics, Rensselaer Polytechnic Institute, Troy, New York

<sup>2</sup>Department of Physics, University of Alabama at Birmingham, Birmingham, Alabama

### Abstract

Beginning with the seminal work of Fritz Zwicky, the existence of dark matter has been one accepted explanation for why orbiting objects in galaxy clusters do not obey the expected Newtonian fall-off with distance. The composition of dark matter has been hypothetically described in several ways, including "Massive Astrophysical Compact Halo Objects" and "Weakly Interacting Massive Particles." This paper explores the possibility that dark matter is actually the relativistic mass associated with the gravitational potential energy ( $U$ ) of these systems, i.e.,  $U/c^2$ . Data were acquired on the orbital velocities and radii of several galaxies, and analysis revealed that  $U$  could be directly related to an integral that could be evaluated solely from that data. The inertial masses for those systems were also extracted from the same data. The calculated inertial masses were in reasonable agreement with published values. However, relativistic masses were found to be five to seven orders of magnitude smaller than inertial masses. Further work is required before a definitive conclusion may be reached, and suggestions for such work are discussed.

### Introduction

The orbital velocities of galaxies do not fall off in the expected Newtonian fashion (as  $1/\sqrt{r}$ ), but rather they approach a constant with increasing radius (Figure 1). Without redefining fundamental laws of nature, this implies that galaxies must contain more mass than we have previously accounted for.<sup>1</sup> There are several possible explanations for this discrepancy. Perhaps the most intriguing involve dark matter (first proposed to exist by Fritz Zwicky in 1933, to explain his own observations of the Coma Cluster<sup>2</sup>), as hypothetically described in terms of Massive Astrophysical Compact Halo Objects (MACHOs)<sup>3,4</sup> and/or Weakly Interacting Massive Particles (WIMPs).<sup>4</sup> Other proposed explanations, including MOND (Modified Newtonian Dynamics)<sup>5</sup>, have involved fundamental modifications of basic equations such as Newton's Law of Gravitation; however, these are outside the scope of this paper.

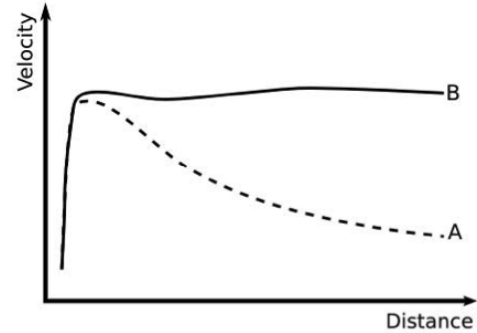


Figure 1. An illustration of the rotation curve of a typical spiral galaxy, where curve A represents the Newtonian prediction and curve B shows the actual observation.

### Theory

In the traditional Newtonian formulation of the orbiting mass in a gravitational field, the centripetal force relation is

$$m \frac{v^2}{r} = G \frac{Mm}{r^2} \quad (1)$$

where  $m$  is the mass of the orbiting object,  $r$  is the distance from the center of orbit,  $v$  is the centripetal velocity, and  $G$  is the universal gravitational constant (approximately  $6.67 \cdot 10^{-11} \text{ N} \cdot \text{m}^2 \cdot \text{kg}^{-2}$ ). Equation 1 simplifies to

$$\frac{v^2}{r} = \frac{GM}{r^2} \rightarrow v^2 = \frac{GM}{r} \quad (2)$$

which leads to the following relationship of the orbital speed  $v$  to the radius  $r$ :

$$v = \sqrt{\frac{GM}{r}} \quad (3)$$

One may also arrive at this relationship using a more general approach based on the Virial Theorem.<sup>6</sup> However, these calculations contradict observations, and this discrepancy led Zwicky to predict the existence of previously unobserved "dark" matter. We approach the problem of calculating the mass of this dark matter in two different ways.

The first method utilizes the following relationship between the centripetal force and the gravitational field:

$$\frac{v^2}{r} = |\vec{g}| = |-\vec{\nabla}\Phi| \quad (4)$$

where the gravitation potential ( $\Phi$ ) associated with the mass density ( $\rho$ ) is given by

$$\Phi = -G \iiint \frac{\rho(\vec{r}')}{|\vec{r} - \vec{r}'|} d^3r' \quad (5)$$

Equation 5 leads to

$$\Phi = -G \iiint \rho(r') Y_{00}(\theta', \phi') \sum_{l=0}^{\infty} \frac{4\pi}{2l+1} \frac{r_{<}^l}{r_{>}^{l+1}} \sum_{m=-l}^l Y_{lm}^*(\theta', \phi') Y_{lm}(\theta, \phi) d\Omega' r'^2 dr' \quad (6)$$

Because  $r$  has a spherical form, the orthonormality of the spherical harmonics reduces the series in  $l, m$  to only the term for  $l = 0, m = 0$ . Thus, Equation 6 becomes

$$\Phi(\vec{r}) = -4\pi G \int_0^{\infty} \rho(r') r'^2 \frac{1}{r_{>}} dr' = -\frac{4\pi}{r} \int_0^r \rho(r') r'^2 dr' - 4\pi \int_r^{\infty} \rho(r') r' dr' \quad (7)$$

By choosing a spherically symmetric form for the dark matter density ( $\rho$ ), such as

$$\rho(r) = \sum_{n=-1}^2 a_n r^n e^{-\alpha_n r} \quad (8)$$

one can indirectly fit the density of matter in the following way. Inserting Equation 8 into Equation 7 results in a closed form for  $\Phi(r)$ . Taking the gradient of this expression and using it in Equation 4 to obtain the specific form that was utilized for this method yields

$$v^2 = 4\pi G \cdot \sum_{n=-1}^2 \left( a_n \cdot \left( \frac{-e^{-\alpha_n r}}{r} \cdot \left( \sum_{b=0}^{(n+2)} (-1)^b \cdot \frac{(n+2)! \cdot r^{(n+2)-b}}{((n+2)-b)! \cdot (-\alpha_n)^{(b+1)}} \right) - \left( \frac{(-1)^{(n+2)}}{r} \cdot \frac{(n+2)!}{(-\alpha_n)^{(n+3)}} \right) \right) \right) \quad (9)$$

Thus, using Equation 9 to fit data for the orbital speeds at different radial distances provides the parameters  $a_n$  and  $\alpha_n$ , which give a fit of the density (Equation 8).

The second method of accounting for the dark matter density is based on the assumption that the dark matter itself is merely the relativistic mass given by the gravitational potential energy ( $U$ ) divided by the square of the speed of light.<sup>7</sup> The gravitational potential energy of the system is given by

$$U = -\frac{G}{2} \cdot \iint \frac{\rho(\vec{r}')\rho(\vec{r})}{|\vec{r} - \vec{r}'|} d^3r' d^3r = -\frac{G}{2} \cdot \int \left( \vec{\nabla} \cdot \left[ (\vec{\nabla}\Phi(\vec{r}))\Phi(\vec{r}) \right] - (\vec{\nabla}\Phi(\vec{r}))^2 \right) dr \quad (10)$$

Using the Poisson equation:

$$\nabla^2\Phi = 4\pi G\rho(\vec{r}) \quad (11)$$

Equation 10 can be rewritten as

$$U = -\frac{1}{8\pi G} \iiint \left( \left[ \vec{\nabla} \cdot (\Phi(\vec{r})\vec{\nabla}\Phi(\vec{r})) \right] - |\vec{g}|^2 \right) d^3r \quad (12)$$

Using the Divergence Theorem  $\iiint_V \vec{\nabla} \cdot \vec{A} d^3\tau = \oiint \vec{A} \cdot \hat{n} dS$ , the first term in Equation 12 turns into a surface integral:  $\oiint (\Phi(\vec{r})\vec{\nabla}\Phi) \cdot \hat{r} dA$ , where  $dA$  is the surface area differential. It is expected that  $(\Phi(\vec{r})\vec{\nabla}\Phi)$  will drop off as  $1/r^3$  while the surface area will grow as  $r^2$ . Thus, for large surface area, this term will go to zero. Under these conditions, the first term of Equation 12 can be neglected. Additionally, by making use of Equation 4, the second term of Equation 12 can be rewritten as

$$U = \frac{1}{8\pi G} \cdot \int_0^\infty 4\pi v^4 dr \quad (13)$$

Yielding the following expression for the mass:

$$\frac{U}{c^2} = mass = \frac{1}{2Gc^2} \cdot \int_0^\infty v^4 dr \quad (14)$$

Then, by using a smooth spline of the data for  $v$ , Equation 14 can be used to obtain values for the inertial mass.

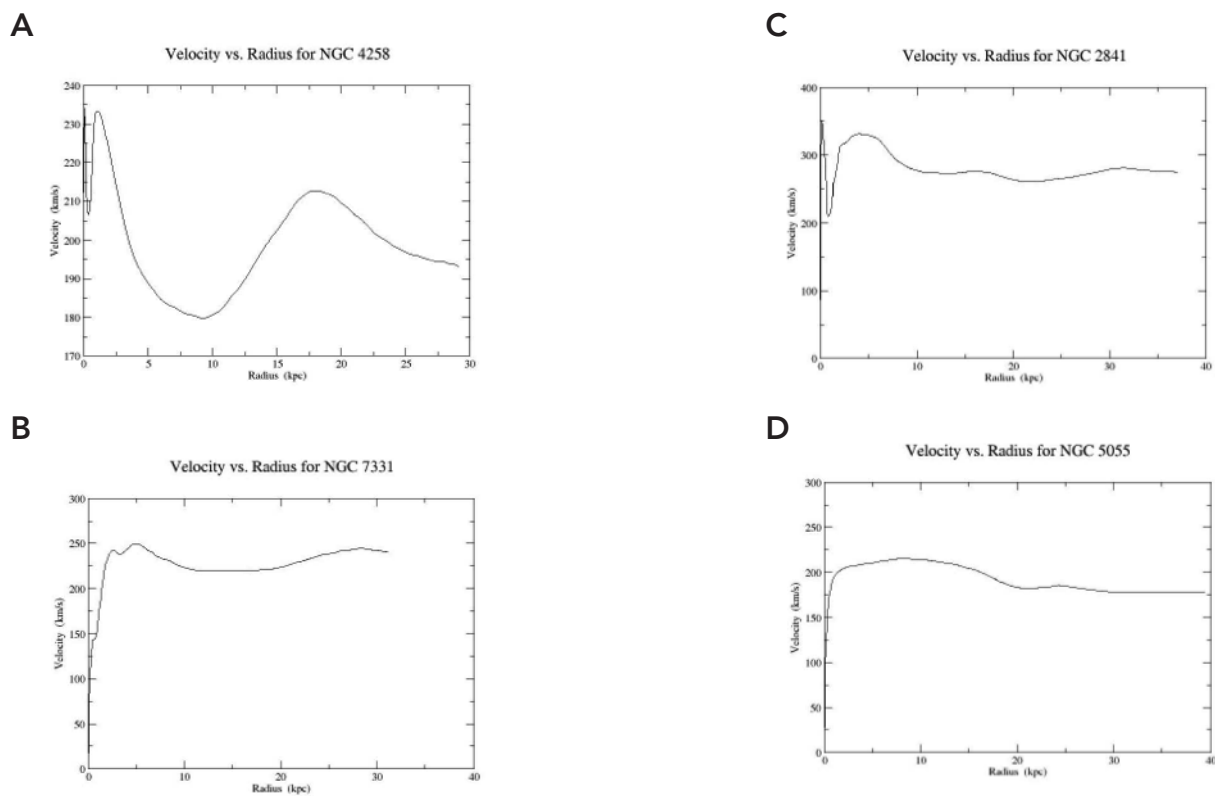


Figure 2. Orbital velocity vs. radius data for four galaxies. These data were manipulated using the fit formulas above. (A) NGC 4258; (B) NGC 7331; (C) NGC 2841; (D) NGC 5055.

## Methods

In order to test the formulas derived herein, we utilized previously collected data relating orbital velocity to radius for several different galaxies (Figure 2).<sup>8</sup>

Non-linear regression analysis techniques were implemented to analyze and acquire fits to the data. First, the orbital velocity vs. radius data were read-in and plotted. A cubic spline was performed on the resulting curve to yield more data points. Then, the orbital velocity data points were squared and plotted against radius. Next, the fit formula (Equation 9) was

applied to the data curve using the non-linear curve fitting command. This process was repeated using different weight factors to achieve better fits. Integrating these fits led to a numerical expression for the mass. The effects of choosing different weighting schemes were analyzed. The number of terms and the weighting factors were both chosen in order to acquire an adequate fit within a reasonable amount of time.

## Results

Figure 3 shows an example of the change in the fit curves when a special weight factor is considered. Table 1

demonstrates how the fit coefficients change when a weight factor is considered. Notice that the fit coefficients change dramatically with different weight factors. Table 2 shows that the effect of the weighting factors on the computed values of the inertial masses is nearly negligible. It is reassuring that the calculated values in Table 2 do not dramatically change with the application of different weight factors. However, there were some unusually small exponential fit coefficients that, when integrated, resulted in an abnormally large masses, thereby indicating an unacceptable fit.

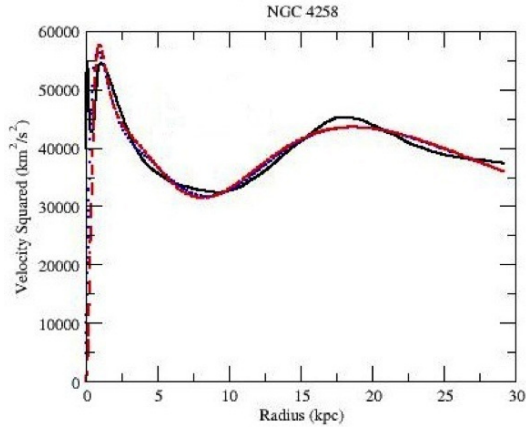


Figure 3. Change in fit curves with application of a weighting factor. The black solid curve is the original data; the blue dotted curve is a fit curve with a weight factor of  $1/y^2$  applied; and the red dashed curve is a fit curve with a weight factor of  $x$  applied.

Table 1. Fit coefficients for NGC 4258 with three different weight factors applied.

Fit Coefficients	Weightings		
	none	$1/y^2$	$x$
$a_0$	415946	7.53622	16553.5
$\alpha_0$	1.84251	0.000168461	0.254778
$a_1$	$5.54981 \times 10^{08}$	12155.1	$9.84164 \times 10^{06}$
$\alpha_1$	$3.19916 \times 10^{06}$	0.374986	5.53256
$a_2$	115.6	-4575.73	-2901.03
$\alpha_2$	0.310573	0.52443	0.586648
$a_3$	$3.11283 \times 10^{06}$	406326	7968.32
$\alpha_3$	16.2339	2.18831	0.53555

Table 2. Effect of weighting factors on the computed values of the inertial masses. The weight factor applied is listed in parentheses. Units are in  $10^{11}$  Solar Masses ( $M_{Sun}$ ).

Galaxy Name	Inertial Mass (none)	Inertial Mass (x)	Inertial Mass ( $x^2$ )	Inertial Mass ( $1/y$ )	Inertial Mass ( $1/y^2$ )
NGC 4258	2.568487	2.53515	2.54748	2.47193	7328308.0*
NGC 7331	90.89388	784450800.0*	3453.271*	27.61070	8.59987
NGC 2841	24.74469	13.07116	12.27777	9.62400	80.72964
NGC 5055	64.67777	80.60132	42172660.0*	452144.7*	3.67188

\*Anomalous results discussed in text.

The relativistic mass plots in Figure 4 have no obvious plateaus. This is indicative of the lack of orbital velocity data beyond that of the luminous matter. Because these plots do not flatten out by 40 kiloparsecs (kpc), we cannot predict what happens to the orbital velocity beyond that radius.

As can be seen in Figure 5, the inertial masses do eventually become relatively constant at a radial distance between approximately 30 and 80 kpc.

It is clear from Figure 6A that between 25 kpc and 30 kpc, there is a crossover of the monotonic increase of the relativistic mass where the inertial mass plateaus. Table 3 gives a side-by-side comparison of the calculated values for both the relativistic mass and the inertial mass of each galaxy.

Table 3. Comparison of relativistic and inertial masses (calculated with no weight factor considered).

Galaxy	Relativistic Mass ( $10^4$ Solar Masses)	Inertial Mass ( $10^{11}$ Solar Masses)
NGC 4258	6.00774	2.56847
NGC 7331	11.24428	90.89388
NGC 2841	30.53165	24.74469
NGC 5055	7.24629	64.67777

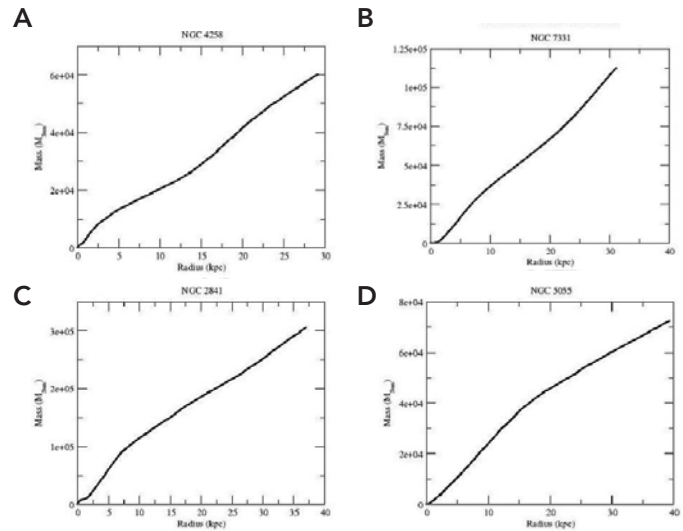


Figure 4. Distribution of the relativistic mass as a function of radius for four galaxies: (A) NGC 4258; (B) NGC 7331; (C) NGC 2841; (D) NGC 5055.

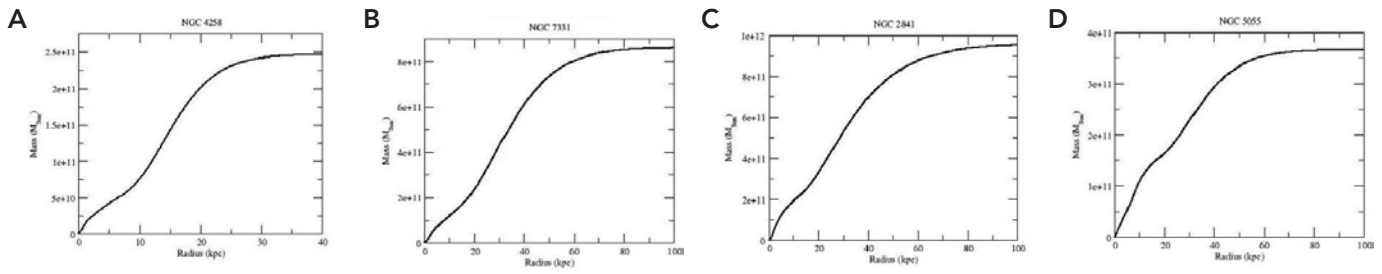


Figure 5. The distribution of the inertial mass as a function of radius for four galaxies: (a) NGC 4258; (b) NGC 7331; (c) NGC 2841; (d) NGC 5055.

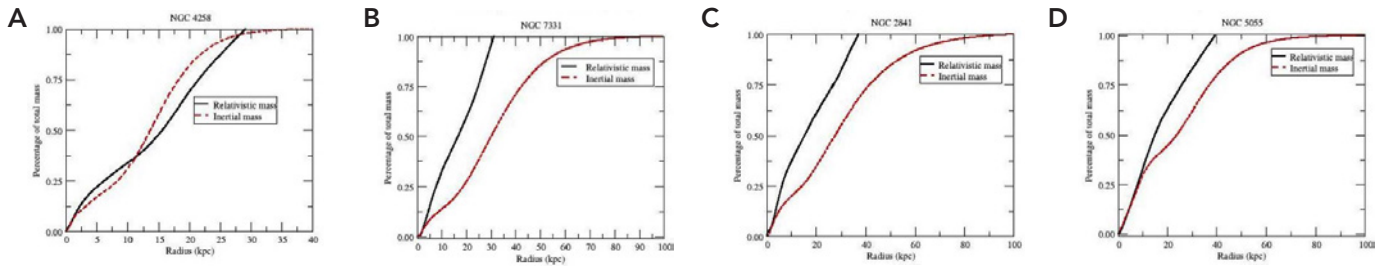


Figure 6. The distribution of the overall mass as a function of radius for four galaxies: (A) NGC 4258; (B) NGC 7331; (C) NGC 2841; (D) NGC 5055.

## Discussion

Einstein's famous mass-energy relation,  $E = mc^2$ , is not simply a relationship between an intrinsic energy and an object's rest mass; that is just a special case of the more general statement. Ascribing inertial properties to an object based on its energy content was an unexpected outcome of Einstein's work with special relativity. It was so groundbreaking and surprising that it prompted Einstein to publish a short comment after his first paper on special relativity.<sup>7</sup> One salient quote from that paper embodies our point: "If a body gives off the energy  $L$  in the form of radiation, its mass diminishes by  $L/c^2$ . The fact that the energy withdrawn from the body becomes energy of radiation evidently makes no difference, so that we are led to the more general conclusion that the mass of a body is a measure of its energy content."

In this study, the energy content of the gravitational field was assessed for its inertial content by integrating the energy density  $\frac{1}{8\pi}|\vec{g}|^2$ . The field strength  $|\vec{g}|$  was inferred from the velocity data for the various galaxies (Equation 4). The shortfall, discussed below, is that velocity data were only available out to a certain radius, and so a proper treatment of the field strength beyond that point could not be obtained.

The fit formula (Equation 9) was first computed for  $n = 0$  through  $n = 2$ . Then, an  $n = -1$  term was added to that interval. Including the  $n = -1$  term allowed the formula to better account for the more rapid change of the density with radius in this region. In the future, addition of an  $n = 3$

term may further improve the fit. The calculations described are limited by the radius of the available data; i.e., we can only compute the mass of the dark matter that is contained within the observed luminous matter halo. Thus if there is a dark matter halo that extends farther from the center of the galaxy than the measured luminous matter halo, then limiting the radius of the data impacts the results. Essentially, the measurement is restricted by the boundary of the luminous matter (Figure 7).

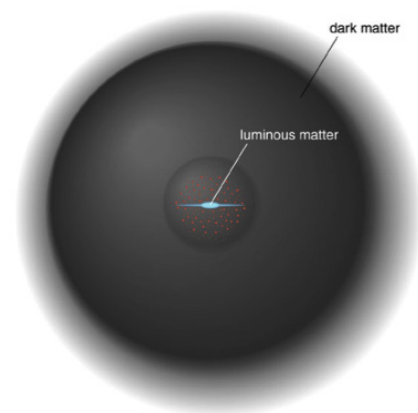


Figure 7. An artist's rendering of a dark matter halo surrounding the luminous matter of a galaxy.<sup>9</sup>

Calculated inertial masses were in agreement with published literature values. Relativistic masses, however, were found to be approximately 5 to 7 orders of magnitude smaller than



inertial masses. Relativistic masses, unlike inertial masses, did not approach asymptotic values. Reaching an asymptotic value implies that the mass density beyond a certain radius is negligible, so that integration beyond that point does not change the value of the total mass. The lack of an asymptotic value for the relativistic masses indicates that our data do not encompass such a radial value. Unfortunately, it is unclear how to evaluate the gravitational potential energy beyond where orbital velocity data are available, unless further assumptions are made. The reason for this is that calculations in this paper were based on orbital velocity data, of which there are no measurements beyond a certain radial extent. It may be possible to solve this issue by fitting the relativistic mass density with a functional form (Equation 14) similar to that of Equation 8, and then integrating the expression to yield relativistic mass.

$$\text{relativistic mass} = \int_0^{\infty} \frac{v^4}{2Gc^2r^2} dr \quad (15)$$

One area of future work will be to apply this analysis to larger systems, such as galaxy clusters.

### Acknowledgments

Support for this research was provided by the National Science Foundation (Grant Number 1058974) Research Experiences for Undergraduates award to UAB. I would also like to thank my mentor, Dr. Joseph Harrison, for allowing me to conduct research under his guidance during the summer program, as well as for his continued guidance and advice after the conclusion of the summer program.

This manuscript was prepared with the AAS LATEX macros v5.2.

### References

- Hibbs, P. (2005). GalacticRotation2.png. Image. Retrieved 15 July 2013 from [www.commons.wikimedia.org/wiki/File:GalacticRotation2.png](http://www.commons.wikimedia.org/wiki/File:GalacticRotation2.png).
- Zwicky, F. (1933). *Helv. Phys. Acta* **6**, 110127. Swiss Physical Society. Translated in *Gen Relativ Gravit* (2009). **41**, 207-224.
- Griest, K. (1990). *Astrophys. J.* **366**, 412-421.
- Griest, K. (1993). *Annals of the New York Academy of Sciences* **688**, 390-407.
- Kroupa, P. et al. (2012). *Int. J. Mod. Phys. D* **21**, 1230003.
- Taylor, J. (2005). *Classical Mechanics*. University Science Books: Sausalito, CA.
- Einstein, A. (1905). Ist die Trägheit eines Körpers von seinem Energiegehalt abhängig? *Annalen der Physik* **18**, 639. Translated in Perrett, W., Jeffrey, G. B. Does the Inertia of a Body Depend on its Energy-Content? Retrieved from [www.fourmilab.ch](http://www.fourmilab.ch).
- Sofue, Y. et al. (1999). *Astrophys. J.* **523**, 136-146.
- Luminous Matter: Diagram. 22-01.jpg. Image. Retrieved 24 July 2013 from [www.physast.uga.edu/~rls/astro1020/ch22/ovhd.html](http://www.physast.uga.edu/~rls/astro1020/ch22/ovhd.html). Image available directly at [www.physast.uga.edu/~rls/1020/ch22/22-01.jpg](http://www.physast.uga.edu/~rls/1020/ch22/22-01.jpg).